

Challenges in XPS Analysis of PEO-LiTFSI-Based Solid Electrolytes: How to Overcome X-Ray-Induced Photodecomposition

Yuriy Yusim,^[a, b] Yannik Moryson,^[a, b] Kevin Seipp,^[c] Joachim Sann,^{*[a, b]} and Anja Henss^{*[a, b]}

The cycle life of poly(ethylene oxide) (PEO) batteries containing lithium bis(trifluoromethanesulfonyl)imide (LiTFSI) is hindered by interfacial (electro)chemical electrolyte decomposition, a process traditionally examined via X-ray photoelectron spectroscopy (XPS). Our research presents a critical examination of X-ray induced photodecomposition, commonly misinterpreted as (electro)chemical electrolyte decomposition, in PEO-LiTFSI systems and those with NCM cathodes. We provide novel insights

into this X-ray induced photodecomposition process and show that it is particularly pronounced when LiTFSI is dissolved and not in its pure state. Most importantly, we reveal that cryogenic measurement conditions can almost completely mitigate this photodecomposition. This insight not only deepens the understanding of photodecomposition within XPS analyses but also provides a transformative approach to the accurate characterization of electrolyte materials in lithium batteries.

1. Introduction

Due to their high energy and power density lithium-ion batteries (LIBs) play a crucial role when it comes to electrochemical energy storage in consumer goods and electric vehicles. Although the energy density has been strongly increased since the LIB commercialization by Sony in 1991,^[1] LIBs with a liquid electrolyte will soon approach a limit in terms of energy density.^[2,3] Thus, potential follow-up systems are under intensive research, such as solid-state batteries (SSBs) with a solid electrolyte (SE).^[4] In this context, solid polymer electrolytes (SPEs) based on poly(ethylene oxide) with lithium bis(trifluoromethanesulfonyl)imide (LiTFSI) as conducting salt were successfully commercialized by Blue Solutions (Bolloré Group).^[5–7] Further, tremendous research efforts have been spent to use PEO-LiTFSI in combination with other SEs in hybrid cell concepts, leading to a layered-like concept^[8,9] or even a three-dimensional mixing^[10,11] to improve the mechanical properties, to increase the lithium-ion conductivity or to lower

the interfacial resistance. Various techniques such as Fourier transform infrared spectroscopy, Raman spectroscopy and X-ray photoelectron spectroscopy (XPS) were used to characterize the interfacial decomposition processes and to study the chemical and electrochemical stability of the polymers in relation to the anode and cathode electrodes. Among these valuable techniques, XPS stands out as particularly advantageous, due to its high surface sensitivity and quantitative nature. For instance, XPS was employed to investigate the interface layer between PEO-based solid polymer electrolytes (SPE) and lithium metal, revealing LiF as a predominant component of the Solid Electrolyte Interphase (SEI).^[12,13] Other polymer host materials, e.g. poly(ϵ -caprolactone) (PCL) and poly(trimethylene carbonate) (PTMC), lead to other electrolyte decomposition phenomena.^[14–16] Further, the interactions between the polymer electrolytes and the conducting salts can lead to the formation of nonequivalent polymer carbons.^[17] These insightful findings support the efficacy of XPS investigations. However, during XPS measurements, X-ray radiation and ion beam sputtering induce various photodecomposition processes, especially when measuring radiation-sensitive samples such as polymer electrolytes. As shown by Shterenberg et al.,^[18] especially the added conducting salts such as magnesium and lithium salts based on TFSI, FSI and PF₆ anions are subject to a significant photodecomposition process during XPS measurements, leading to the formation of new peaks with lower binding energy (BE) in the fluorine and sulphur XP spectra. In this context, the signal appearing in the XP spectrum of F 1s at about 685 eV,^[19,20] can be attributed to the formation of LiF species. These results were confirmed by Yu et al.^[21] who emphasized that any residual salt in the electrode sample during XPS analysis is likely to generate LiF, regardless of battery operation. Studying the actual (electro)chemical electrolyte decomposition of the conducting salt within a polymer matrix is challenging, and XPS analysis data can be susceptible to misinterpretation due to X-ray induced photodecomposition, potentially leading to erroneous

[a] Y. Yusim, Y. Moryson, J. Sann, A. Henss
Institute of Physical Chemistry, Justus Liebig University Giessen, Heinrich-Buff-Ring 17, 35392 Giessen, Germany
E-mail: Joachim.Sann@phys.chemie.uni-giessen.de
Anja.Henss@phys.chemie.uni-giessen.de

[b] Y. Yusim, Y. Moryson, J. Sann, A. Henss
Center for Materials Research (ZfM/LaMa), Justus Liebig University Giessen, Heinrich-Buff-Ring 16, 35392 Giessen, Germany

[c] K. Seipp
Department of Chemistry, Johannes Gutenberg University, Duesbergweg 10–14, 55128 Mainz, Germany

 Supporting information for this article is available on the WWW under <https://doi.org/10.1002/batt.202400161>

 © 2024 The Authors. Batteries & Supercaps published by Wiley-VCH GmbH. This is an open access article under the terms of the Creative Commons Attribution Non-Commercial NoDerivs License, which permits use and distribution in any medium, provided the original work is properly cited, the use is non-commercial and no modifications or adaptations are made.

conclusions, as recently shown by Misuse et al. For example, Hobold et al.^[22] reported an overestimation of LiF content in the SEI on lithium metal. Although lithium salt photodecomposition has been extensively reported in the literature, there is a critical need to assess its impact and to formulate effective mitigation strategies. This is important to ensure the accuracy of XPS analysis in future studies.

Therefore, in this study, we have carried out an exemplary analysis of PEO-based solid polymer electrolytes (SPEs) and their interfacial properties in conjunction with nickel cobalt manganese oxide (NCM) using X-ray photoelectron spectroscopy (XPS). By collecting XP surface spectra for PEO-LiTFSI and PEO-LiTFSI in contact with NCM, we observed a significant increase in LiF content with prolonged X-ray exposure time, indicating X-ray photodecomposition. To mitigate beam damage and ensure accurate surface analysis, rapid measurements and cryogenic conditions were employed, which effectively slowed the rate of lithium salt photodecomposition. Despite these measures, our comprehensive results did not support the presence of LiF-containing decomposition products in pristine PEO-LiTFSI or PEO-LiTFSI in contact with NCM.

Experimental Section

Materials

Poly(ethylene oxide) (PEO, $M_w = 8,000,000 \text{ g mol}^{-1}$) and 1-methyl-2-pyrrolidone (NMP, anhydrous, 99.5%) were purchased from Sigma-Aldrich. Lithium bis(trifluoromethanesulfonyl)imide (LiTFSI, 99.9%), Lithium bis(fluorosulfonyl)imid (LiFSI, > 98.0%) and polyvinylidene difluoride (PVDF, Solef 5130) were purchased from Solvay, the conductive carbon (Super P) from Timcal and single crystalline $\text{LiNi}_{0.83}\text{Co}_{0.11}\text{Mn}_{0.06}\text{O}_2$ was purchased from MSE Supplies. Lithium metal (thickness: 60 μm , Honjo, Japan) was used as counter electrode. The siliconized polyester foil (thickness: 100 μm) was purchased from Valentia Industries LTD, Ireland and pouch bag foil from Showa Denko, Japan. All chemicals and cell components were dried under vacuum before use. In particular, PEO was vacuum dried at 50 °C for 72 hours, according to literature.^[8] Material storage were carried out in an argon-filled glovebox (<0.1 ppm of O₂, <0.1 ppm of H₂O).

PEO Membrane Preparation^[5,23]

Free-standing PEO-LiTFSI membranes ($M_w = 8,000,000 \text{ g mol}^{-1}$) were prepared by a solvent-free technique in order to exclude any solvent related effect.^[24] For this reason, 1000 mg of PEO and 650 mg of LiTFSI (EO/Li ratio 10:1) were mixed until the powders formed a sticky composite, which was placed between two siliconized polyester foils, transferred into an aluminum-laminated pouch bag, vacuum sealed (Sealervac) and annealed for 12 h at 90 °C. Then the pouch bag with the polymer electrolyte was hot-pressed (Atlas™ Series Autotouch) between two metal plates at 90 °C with 294 MPa for 10 s. To prepare the SPE for XPS analysis, the membrane was punched into pieces. For the preparation of PEO-LiFSI, 1000 mg PEO and 419 mg LiFSI were mixed (EO/Li ratio 10:1) and the same procedure was followed, however, the mixture was not pressed, but cut into pieces.

Electrode Preparation and Cell Assembly

Electrode preparation and cell assembly are described in our previous work.^[5,23]

XPS Measurements

X-ray photoelectron spectroscopy (XPS) measurements were performed using a PHI5000 Versa Probe IV (Physical Electronics GmbH) with an aluminum anode (Al K α = 1486.6 eV). The X-ray power and beam diameter were 50 W and 200 μm , respectively. The pass energy of the analyzer was set to 112 eV to obtain the survey and 27 eV to obtain detail spectra. The samples were transferred with an argon-filled transfer module. The samples were mounted on insulating double sided tape, thus the samples were neutralized during the measurement with the PHI dual beam neutralization consisting of a low current of 10 eV Ar⁺ ions and 5 μA of 1eV electrons, fixing the potential during the measurements at -1 V vs ground level. XPS data evaluation was carried out with CasaXPS (Version 2.3.23PR1.0). All spectra were calibrated in relation to the F 1s -CF₃ signal at 688.7 eV.

2. Results and Discussion

In this study, we focused on the analysis of the PEO-LiTFSI | NCM interface using X-ray photoelectron spectroscopy (XPS). Current literature indicates that the interface in PEO-based SSBs with high voltage cathodes is significantly more unstable compared to the interface on the anode side.^[23,25,26] Thus, we focused firstly on this interface and designed a Li|PEO-LiTFSI|LiNi_{0.83}Mn_{0.06}Co_{0.11}O₂/PVDF/Super P cell, which is a very standard system according to common literature.^[5,27,25] The cell was stored at 80 °C to facilitate partial infiltration of the cathode with PEO-LiTFSI. The aluminum current collector was then removed from the cathode and XPS analysis was performed on the surface facing the current collector. It is important to emphasize that our XPS measurements followed the established methodologies commonly used and described in the literature, including the prescribed measurement procedure and duration. Figure 1a shows the F 1s spectrum containing the -CF₃ group of LiTFSI and -CF₂ of PVDF at 688.7 eV. The adjacent LiF signal at 684.8 eV is often associated with a (electro)chemical decomposition product of LiTFSI in the existing literature.^[19] For example, previous studies have reported the formation of a LiF-containing reaction layer when depositing PEO-LiTFSI ($M_w = 2,000 \text{ g mol}^{-1}$) on LCO thin films.^[28] Other researchers^[29] have also suggested that the (electro)chemical decomposition of PEO-LiTFSI could occur already at 3.2 V (vs. Li⁺/Li), which is close to the open circuit potential of NCM against Li.^[30] Taken together, these reports could provide a plausible explanation for the observation of the LiF signal in the XP spectrum when PEO-LiTFSI is in contact with NCM. To further investigate whether LiF is a (electro)chemical decomposition product, we performed XPS measurements on untreated PEO-LiTFSI as a reference (Figure 1b). Therefore, free-standing PEO-LiTFSI membranes were prepared (see PEO membrane preparation, experimental section). Interestingly, in these measurements (no PVDF present in these samples) we observed a LiF signal of

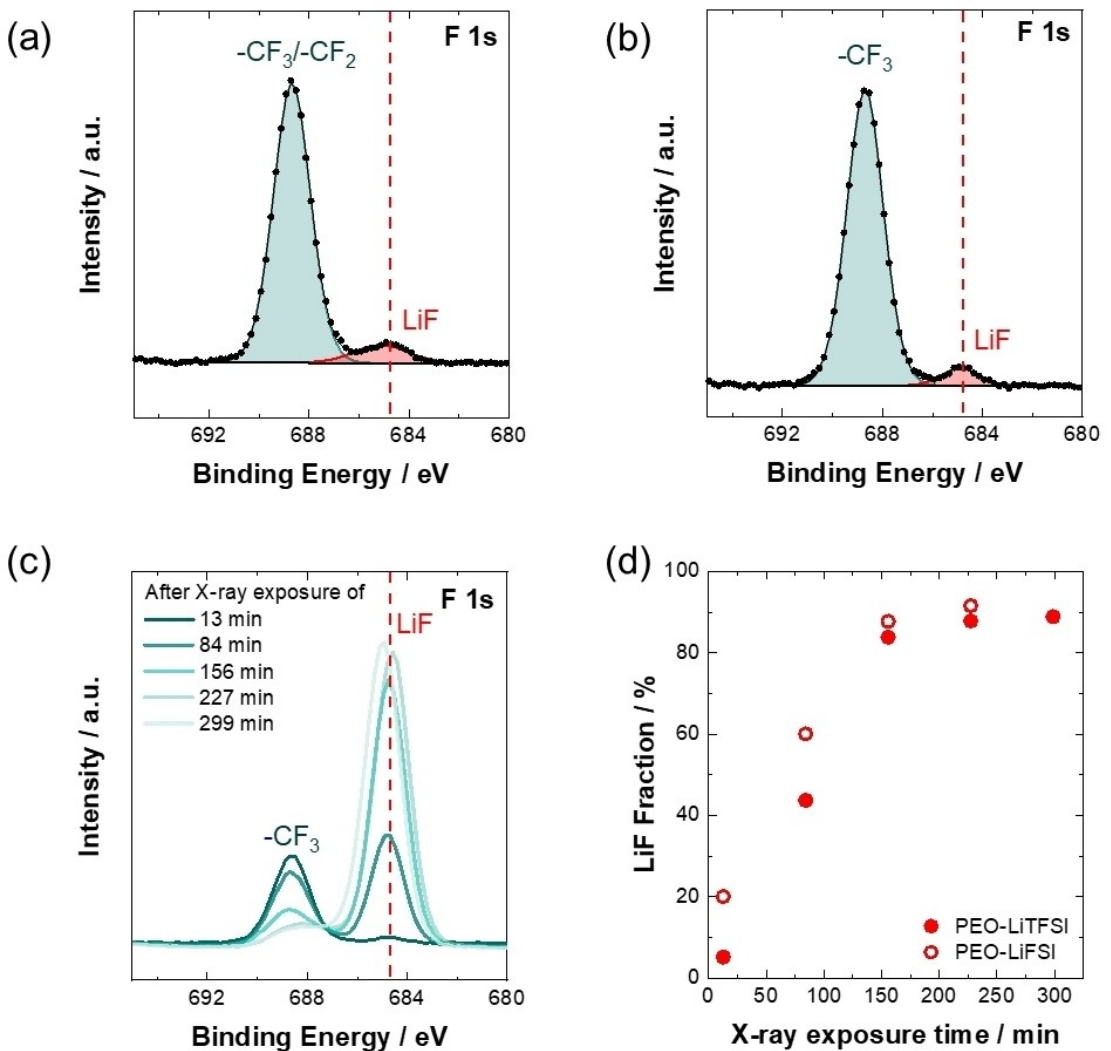


Figure 1. F 1s XP spectra of (a) PEO-LiTFSI in contact with NCM cathode and (b) pure PEO-LiTFSI. (c) PEO-LiTFSI after X-ray exposure for 13, 84, 156, 227 and 299 min, respectively. (d) LiF fraction as function of the X-ray exposure time for PEO-LiTFSI and PEO-LiFSI.

comparable intensity as in measurements on PEO-LiTFSI that had been in contact with the NCM cathode. Accordingly, we assume the LiF signal is not mainly from PVDF, which is present in the cathode. In a previous study by Simon et al.,^[10] LiF was also detected in “pristine” PEO-LiTFSI in XP spectra. This raises the question of whether LiF is actually a (electro)chemical decomposition product or an artefact of the measurement procedure, in particular the X-ray decomposition investigated below.

In our investigation, we observed a significant trend in line with the studies by Shterenberg et al.,^[18] Högström^[31] and Breuer et al.^[32] Upon multiple measurements of the identical PEO-LiTFSI position and an increase in X-ray exposure time (an X-ray exposure of 13 min leads to an energy dose of $1.2 \cdot 10^7 \text{ J cm}^{-2}$), a remarkable increase in the LiF content within PEO-LiTFSI was evident. This was accompanied by a corresponding decrease in the $-\text{CF}_3$ content, as shown in Figure 1c. A similar trend was observed for PEO-LiFSI (see Figure S4). To quantify these changes, the relative fraction of LiF in the total F

1s spectrum, derived from fitting the XP spectra, was plotted against X-ray exposure time in Figure 1d. The graph shows an initial linear increase in the LiF fraction, which plateaued at a relative amount of 80–90% LiF fraction for PEO-LiTFSI and PEO-LiFSI, respectively. Consequently, it is evident that the LiF signal is highly susceptible to X-ray photodecomposition. Furthermore, we ruled out a significant influence of the high vacuum in the chamber on the decomposition of the conducting salt, as repeating the experiment after extended pumping times (12 hours) yielded the same results.

We conducted additional XPS detail spectra measurements in varying sequences. Specifically, we compared the F 1s spectrum of PEO-LiTFSI recorded initially (see Figure 1b) against that recorded after recording other element regions (survey, C, O, Li, S, N). Figure S1 shows a significant reduction in LiF content, from 53% to 5%, when the F 1s spectrum is measured first. This supports our findings on LiTFSI’s photodecomposition during XPS analysis. These experiments highlight the criticality of assessing battery sample sensitivity to radiation damage and

monitoring rate changes for a reliable and consistent measurement protocol. Moreover, they underline the necessity of uniform analysis duration and procedures across samples to ensure consistent X-ray exposure, as suggested by Philippe et al.^[33] in their research.

To address the above question of whether LiF is a genuine (electro)chemical decomposition product or an artefact of the measurement, it is important to consider the observed instability of the PEO-LiTFSI samples under X-ray radiation. With this in mind, it can be hypothesised that the LiF signal found in the XP spectra of both pristine PEO-LiTFSI and PEO-LiTFSI in contact with NCM is primarily due to X-ray photodecomposition during the XPS measurement rather than (electro)chemical decomposition.

Moving forward, our focus is shifting to exploring methods that can mitigate the artefact of X-ray decomposition. This effort is aimed at validating the earlier hypothesis and providing a robust basis for reliable XPS analysis in subsequent studies. As part of this effort, we have minimised the number of scans required to obtain the XP spectrum.^[34] Instead of the 35 scans (dose: $1.2 \cdot 10^7 \text{ J cm}^{-2}$) used for the measurement depicted in Figure 1, we performed a measurement with a single scan (dose: $3.4 \cdot 10^5 \text{ J cm}^{-2}$). It is important to note, that while the signal quality improves with increasing number of scans, the radiation damage becomes more pronounced. Using a single scan, no LiF-signal can be detected at 685 eV for PEO-LiTFSI (Figure 2a) and for PEO-LiTFSI in contact with NCM (Figure 2b) indicating the absence of LiTFSI decomposition to LiF in both samples. Similar results were obtained, when cell was charged

to 4.3 V vs. Li^+/Li and the potential was held at 4.3 V for 45 h, to accelerate the electrochemical electrolyte decomposition (see Figure S2). Accordingly, the electrochemical electrolyte decompositions of PEO-based SPE seems not to lead to the formation of LiF species. However, the oxidative degradation of PEO-based SPEs with high voltage is beyond the scope of this work and was examined in our previous studies.^[23,5]

To improve the signal-to-noise ratio, XP spectra were collected at 48 different points on the surface of the PEO-LiTFSI with one scan each (analysis areas did not overlap), and subsequently summed, confirming the absence of LiF (see Figure 2c). Overall, it can be concluded that the LiF signal in pristine PEO-LiTFSI and PEO-LiTFSI in contact with NCM is a consequence of X-ray radiation damage and not (electro)chemical decomposition. In addition, when pure LiTFSI is measured no increase in chamber pressure was observed and no gas release was detected by mass spectrometry, ruling out the formation of gaseous products during photodecomposition, contrary to the findings of Shterenberg et al.^[18] It is important to acknowledge that we do not completely exclude the possibility that PEO-LiTFSI may undergo various decomposition reactions when in contact with NCM. In addition, our results have limited comparability with the findings of Ferber et al.,^[28] who observed the decomposition of PEO-LiTFSI in contact with LCO. A notable difference in their study is the use of LCO instead of NCM as the cathode material. In addition, our NCM materials are coated, similar to many commercially available cathode active materials. It is well known that coatings can play

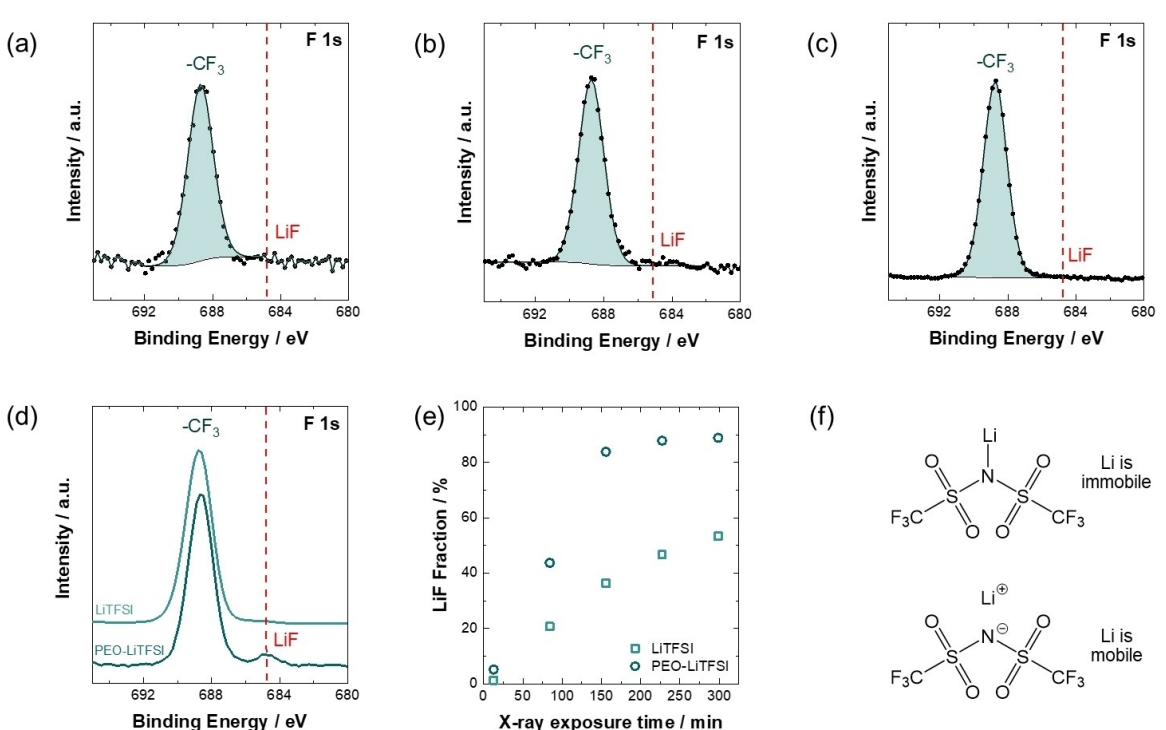


Figure 2. XP F 1s spectra using one scan of (a) PEO-LiTFSI and (b) PEO-LiTFSI in contact with NCM cathode. (c) Summed F 1s XP spectra using one scan from 48 different surface points of PEO-LiTFSI (d) Comparison of XP spectra of PEO-LiTFSI and pure LiTFSI powder. (e) LiF fraction as function of the X-ray exposure time for PEO-LiTFSI and LiTFSI. (f) Schematic comparison of the structure of pure LiTFSI and LiTFSI dissolved in PEO.

a role in mitigating decomposition at the interface between the cathode material and the SPE.

In addition, an XP surface spectrum of pure LiTFSI was collected and compared to the PEO-LiTFSI using the same measurement procedure (sum of 35 scans, dose: $1.2 \cdot 10^7 \text{ J cm}^{-2}$). As shown in Figure 2d, only a small fraction of LiF (< 1.2%) can be detected on the surface of pure LiTFSI. Moreover, the observed X-ray decomposition over time shows differences between pure LiTFSI and PEO-LiTFSI (see Figure 2d). Corresponding to the surface spectra in Figure 2c, it appears that the X-ray decomposition is more pronounced, when LiTFSI is dissolved in the PEO-matrix compared to pure LiTFSI as shown in Figure 2e. To ensure the reliability of our results, we repeated this trend with LiFSI and PEO-LiFSI (see Figure S3). These data indicate that the X-ray photodecomposition of conducting salts differs whether they are ionically bonded in the pure solid state or dissolved. Considering the structure of LiTFSI, a possible explanation for this behavior may lie in the increased mobility of the lithium cation when LiTFSI is dissolved, potentially bringing it into closer proximity with the $-\text{CF}_3$ group (see Figure 2f). This increases the probability of collision between the $-\text{CF}_3$ group and the Li cation, leading to the formation of LiF. These overall findings can be supported by Marchiori et al.,^[35] who performed thermodynamic calculations based on atomic-scale modeling to assess the electrochemical stability window (ESW) of LiTFSI and of PEO-LiTFSI. Interestingly, they observed a significant narrowing of the ESW in the PEO/LiTFSI complex compared to pure LiTFSI. The lowering of the oxidation potential is caused by the oxidative deprotonation of PEO in the PEO/FSI⁻ complex. Accordingly, in agreement with the photodecomposition observations in this study, the stability of conducting salt can change when polymer/salt complex is formed.

It is important to highlight that a recent paper^[32] demonstrated complementary results to those we observed. They also showed a rapid photodecomposition of PEO-LiTFSI to LiF. Additionally, they found that the X-ray decomposition of LiTFSI in a PEO matrix is more pronounced than in pure LiTFSI, which is in good agreement with our work. Overall, their results support findings at room temperature.

Given the apparent dependence of the photodecomposition rate of LiTFSI to LiF on the mobility of lithium cations (as discussed earlier), we performed XPS measurements on PEO-LiTFSI under cryogenic conditions to slow down the kinetics of the X-ray induced decomposition reaction. In contrast to the room temperature measurements of PEO-LiTFSI shown in Figure 1b, no LiF-signal is detectable when the XP spectra are collected at -130°C (see Figure 3). This suggests that the X-ray induced decomposition of LiTFSI into LiF can be mitigated when measurements are performed at low temperatures. To ensure the robustness of our results, we repeated the same experiment with PEO-LiFSI and obtained similar results (see Figure S5). This further confirms that no decomposition occurred between PEO and LiTFSI and supports the validity of our conclusion. Overall, the strong temperature dependence of the photodecomposition process observed in dissolved LiTFSI suggests that the key reaction step is controlled by transport

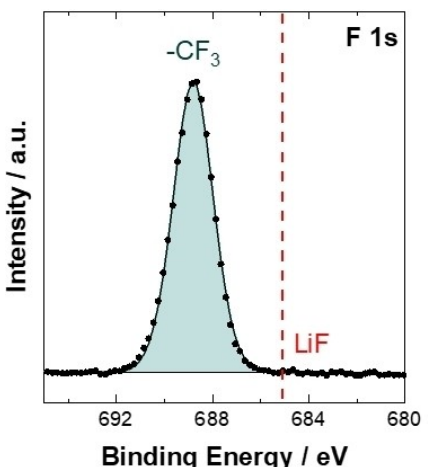


Figure 3. F 1s XP spectrum of PEO-LiTFSI measured under cryogenic conditions (-130°C).

phenomena. We hypothesize that due to the photoelectronic effect, an electron from the nitrogen of the LiTFSI/LiFSI may be removed, possibly leading to an intermolecular or intramolecular reduction of the CF_3 group in subsequent steps (see Figure S6). The latter process may be similar to the CF_4 gas-phase reaction mechanisms reported by Zhang et al.,^[36] who studied plasma-surface reactions in fluorocarbon plasmas and simulated potential CF_4 gas-phase reaction mechanism. As a side note, X-ray beam damage presented in this study is not only limited to X-ray spectroscopy. It is well known that prolonged radiation exposure during X-ray diffraction can lead to macroscopic consequences such as amorphization and swelling.^[37,38]

3. Conclusions

In this study, we emphasize the critical importance of X-ray induced photodecomposition in PEO-LiTFSI. We demonstrate that the influence of photodecomposition can be significantly decreased either by (a) minimizing X-ray exposure times through clever design of the XPS experiment or (b) by applying cryogenic conditions during the measurement. We specifically want to highlight the second approach, since in our experiments cryogenic conditions allowed for vastly higher X-ray-doses without significant decomposition, which significantly improved the signal-to-noise-ratios.

Our results provide new insights into the photodecomposition process, in particular highlighting the likely influence of transport phenomena in the key reaction step. Based on this understanding, we observed no LiF-containing (electro)-chemical decomposition products in pristine PEO-LiTFSI and PEO-LiTFSI in contact with NCM, challenging certain existing claims in the literature. Overall, our study improves the understanding of X-ray photodecomposition and suggests effective strategies for performing reliable XPS analysis.

Supporting Information

Experimental section; F 1s XP spectrum of PEO-LiTFSI after other elements were measured; F 1s XP spectrum of cathode after high voltage exposure; PEO-LiTFSI after different X-ray exposure times; LiF fraction as function of X-ray exposure time for PEO-LiTFSI and LiFSI; F 1s XP spectrum of PEO-LiTFSI at RT and cryogenic conditions; Suggested mechanism of X-ray photo-decomposition.

Author Contributions

Y.Y., A.H. and J.S. conceived the idea. A.H. and J.S. supervised all aspects of the research. Y.Y. carried out the XPS measurements including the sample preparation. Y.M. and K.S. supported in the interpretation and analysis of measured data. Y.Y. wrote the first draft of the manuscript. All authors revised and approved the manuscript.

Acknowledgements

The authors would like to acknowledge the financial support from the Federal Ministry of Education and Research (BMBF) within the FestBatt 2 Hybrid (03XP0428E), the FestBatt 2 Characterisation (03XP0433D) and the ProGral (03XP0427) projects. A.H. would like to thank the "Professorinnenprogramm III" funded by BMBF. Open Access funding enabled and organized by Projekt DEAL.

Conflict of Interests

The authors declare no competing financial interest.

Data Availability Statement

The data that support the findings of this study are available from the corresponding author upon reasonable request.

Keywords: XPS • Cryogenic conditions • Solid polymer electrolytes • Poly(ethylene oxide) (PEO) • Conducting salts • Interface stability

- [1] M. V. Reddy, A. Mauger, C. M. Julien, A. Paolella, K. Zaghib, *Materials* **2020**, *13*, 1884.
- [2] J. Janek, W. G. Zeier, *Nat. Energy* **2016**, *1*, 16141.
- [3] J. Janek, W. G. Zeier, *Nat. Energy* **2023**, *8*, 230.
- [4] R. S. Negi, Y. Yusim, R. Pan, S. Ahmed, K. Volz, R. Takata, F. Schmidt, A. Henss, M. T. Elm, *Adv. Mater. Interfaces* **2022**, *9*, 2270039.
- [5] Y. Yusim, E. Trevisanello, R. Ruess, F. H. Richter, A. Mayer, D. Bresser, S. Passerini, J. Janek, A. Henss, *Angew. Chem. Int. Ed.* **2023**, *62*, e202218316.
- [6] A. Varzi, R. Raccichini, S. Passerini, B. Scrosati, *J. Mater. Chem. A* **2016**, *4*, 17251.

- [7] H. Huo, M. Jiang, B. Mogwitz, J. Sann, Y. Yusim, T.-T. Zuo, Y. Moryson, P. Minnmann, F. H. Richter, C. Veer Singh, J. Janek, *Angew. Chem. Int. Ed.* **2023**, *62*, e202218044.
- [8] F. J. Simon, M. Hanauer, A. Henss, F. H. Richter, J. Janek, *ACS Appl. Mater. Interfaces* **2019**, *11*, 42186.
- [9] S.-S. Chi, Y. Liu, N. Zhao, X. Guo, C.-W. Nan, L.-Z. Fan, *Energy Storage Mater.* **2019**, *17*, 309.
- [10] F. J. Simon, M. Hanauer, F. H. Richter, J. Janek, *ACS Appl. Mater. Interfaces* **2020**, *12*, 11713.
- [11] Y. Zhao, Z. Huang, S. Chen, B. Chen, J. Yang, Q. Zhang, F. Ding, Y. Chen, X. Xu, *Solid State Ionics* **2016**, *295*, 65.
- [12] I. Ismail, A. Noda, A. Nishimoto, M. Watanabe, *Electrochim. Acta* **2001**, *46*, 1595.
- [13] C. Xu, B. Sun, T. Gustafsson, K. Edström, D. Brandell, M. Hahlin, *J. Mater. Chem. A* **2014**, *2*, 7256.
- [14] E. K. W. Andersson, C. Sångeland, E. Berggren, F. O. L. Johansson, D. Kühn, A. Lindblad, J. Mindemark, M. Hahlin, *J. Mater. Chem. A* **2021**, *9*, 22462.
- [15] C. Sångeland, G. Hernández, D. Brandell, R. Younesi, M. Hahlin, J. Mindemark, *ACS Appl. Mater. Interfaces* **2022**, *14*, 28716.
- [16] B. Sun, C. Xu, J. Mindemark, T. Gustafsson, K. Edström, D. Brandell, *J. Mater. Chem. A* **2015**, *3*, 13994.
- [17] D. Martin-Vossrage, B. V. R. Chowdari, *J. Electrochem. Soc.* **1995**, *142*, 1442.
- [18] I. Shertenberg, M. Salama, Y. Gofer, D. Aurbach, *J. Phys. Chem. C* **2017**, *121*, 3744.
- [19] M. R. Busche, T. Drossel, T. Leichtweiss, D. A. Weber, M. Falk, M. Schneider, M.-L. Reich, H. Sommer, P. Adelhelm, J. Janek, *Nat. Chem.* **2016**, *8*, 426.
- [20] Z. Huang, J. Meng, M. Xie, Y. Shen, Y. Huang, *J. Mater. Chem. A* **2020**, *8*, 14198.
- [21] W. Yu, Z. Yu, Y. Cui, Z. Bao, *ACS Energy Lett.* **2022**, *7*, 3270.
- [22] G. M. Hobold, B. M. Gallant, *ACS Energy Lett.* **2022**, *7*, 3458.
- [23] Y. Yusim, D. F. Hunstock, A. Mayer, D. Bresser, S. Passerini, J. Janek, A. Henss, *Adv. Mater. Interfaces* **2023**, *11*(3), 2300532.
- [24] G. B. Appetecchi, M. Carewska, F. Alessandri, P. P. Prosini, S. Passerini, *J. Electrochem. Soc.* **2000**, *147*, 451.
- [25] J. Qiu, X. Liu, R. Chen, Q. Li, Y. Wang, P. Chen, L. Gan, S.-J. Lee, D. Nordlund, Y. Liu, X. Yu, X. Bai, H. Li, L. Chen, *Adv. Funct. Mater.* **2020**, *30*(22), 1909392.
- [26] Y. Liu, Y. Zhao, W. Lu, L. Sun, L. Lin, M. Zheng, X. Sun, H. Xie, *Nano Energy* **2021**, *88*, 106205.
- [27] G. Homann, L. Stoltz, J. Nair, I. Cekic Laskovic, M. Winter, J. Kasnatscheew, *Sci. Rep.* **2020**, *10*, 4390.
- [28] T. H. Ferber, Ş. Cangaz, W. Jaegermann, R. Hausbrand, *Appl. Surf. Sci.* **2022**, *571*, 151218.
- [29] L. Seidl, R. Grissa, L. Zhang, S. Trabesinger, C. Battaglia, *Adv. Mater. Interfaces* **2022**, *9*, 2100704.
- [30] J. Schmalstieg, C. Rahe, M. Ecker, D. Uwe Sauer, *J. Electrochem. Soc.* **2018**, *165*, A3799–A3810.
- [31] K. C. Höglström, *Doctoral thesis 2014*, Uppsala University.
- [32] O. Breuer, Y. Gofer, Y. Elias, M. Fayena-Greenstein, D. Aurbach, *J. Electrochem. Soc.* **2024**, *171*, 30510.
- [33] B. Philippe, M. Hahlin, K. Edström, T. Gustafsson, H. Siegbahn, H. Rensmo, *J. Electrochem. Soc.* **2016**, *163*, A178–A191.
- [34] S. Malmgren, K. Ciosek, R. Lindblad, S. Plogmaker, J. Kühn, H. Rensmo, K. Edström, M. Hahlin, *Electrochim. Acta* **2013**, *105*, 83.
- [35] C. F. N. Marchiori, R. P. Carvalho, M. Ebadi, D. Brandell, C. Moyses Araujo, *Chem. Mater.* **2020**, *32*, 7237.
- [36] Da Zhang, M. J. Kushner, *J. Vac. Sci. Technol. A* **2000**, *18*, 2661.
- [37] A. Boulle, A. Chartier, J.-P. Crocombette, T. Jourdan, S. Pellegrino, A. Debelles, *Nucl. Instrum. Methods Phys. Res., B* **2019**, *458*, 143.
- [38] R. N. Widmer, G. I. Lampronti, N. Casati, S. Farsang, T. D. Bennett, S. A. T. Redfern, *Phys. Chem. Chem. Phys.* **2019**, *21*, 12389.

Manuscript received: March 7, 2024
Revised manuscript received: June 14, 2024
Accepted manuscript online: June 20, 2024
Version of record online: August 19, 2024